

# Investigation of (n,x) reactions on enriched Ge targets at 15.7 MeV at the upgraded facility of NCSR "Demokritos"

S. Chasapoglou<sup>1,\*</sup>, R. Vlastou<sup>1</sup>, M. Diakaki<sup>1</sup>, M. Kokkoris<sup>1</sup>, L. Amanatidis<sup>1</sup>, M. Axiotis<sup>2</sup>, S. Harissopoulos<sup>2</sup>, and A. Lagoyannis<sup>2</sup>

<sup>1</sup>Department of Physics, National Technical University of Athens, Zografou Campus, Athens, 15772, Greece

<sup>2</sup>Tandem Accelerator Laboratory, Institute of Nuclear and Particle Physics, N.C.S.R. Demokritos, Athens, 15341, Greece

**Abstract.** Neutron induced reaction cross-section measurements display special interest both for fundamental research in the Nuclear Physics field and many practical applications. The Institute of Nuclear and Particle Physics (INP) of the National Centre for Scientific Research Demokritos (N.C.S.R. "D") hosts the 5.5 MV T11/25 Van de Graaff accelerator, which is the only accelerator used in Greece for research purposes. This accelerator recently underwent a major upgrade, including the installation of a new pelletron charging system, two new ion sources, a new gas stripper and beam optics. This neutron facility can produce quasi-monoenergetic neutron beams in the energy range  $\sim$ 16-19 MeV via the  $^3\text{H}(\text{d},\text{n})^4\text{He}$  (D-T) reaction, employing a tritiated Titanium target (TiT). The neutron induced cross sections of a total of nine reaction channels have been experimentally measured in the present work, via the activation technique, using enriched Ge targets. These targets produce more accurate cross-section results, in comparison with the - most commonly used in bibliography -  $^{nat}\text{Ge}$  samples, since they do not suffer from contaminating reactions that produce the same residual nucleus. Monte Carlo simulations were also performed via the combined use of MCNP5 and NeuSDesc codes for the simulation of the neutron beam.

## 1 Introduction

The study of neutron induced reactions on Ge isotopes is very important for practical applications such as dosimetry, nuclear medicine, astrophysical projects and reactor technology [1-3]. Ge is also very widely used as a constructional material for  $\gamma$ -ray detectors. For fundamental research, the study of neutron induced reactions on the five natural occurring isotopes of Ge ( $^{70,72,73,74,76}\text{Ge}$ ) can lead to very interesting systematics. Moreover, the residual nuclei from some reaction channels, are produced in high spin isomeric states, with the corresponding decays being heavily dependent on the spin distribution of the continuum phase-space, and the spins of the discrete levels involved. The accurate cross-section measurement of such reactions is thus very important for the study of the residual nucleus [1, 4, 5]. In addition, at energies above 15 MeV, pre-equilibrium effects in the de-excitation of the compound nucleus become more important [1] and accurate cross-section data in this energy region as the

\* e-mail: [sotirischasapoglou@mail.ntua.gr](mailto:sotirischasapoglou@mail.ntua.gr)

ones produced with enriched targets, could vastly improve the accuracy of statistical model calculations and future evaluation libraries.

In this scope, the cross sections of the  $^{70}\text{Ge}(\text{n},2\text{n})^{69}\text{Ge}$ ,  $^{72}\text{Ge}(\text{n},\text{p})^{72}\text{Ga}$ ,  $^{72}\text{Ge}(\text{n},\alpha)^{69\text{m}}\text{Zn}$ ,  $^{73}\text{Ge}(\text{n},\text{p})^{73}\text{Ga}$ ,  $^{73}\text{Ge}(\text{n},\text{np/d})^{72}\text{Ga}$ ,  $^{73}\text{Ge}(\text{n},\text{n}\alpha)^{69\text{m}}\text{Zn}$ ,  $^{74}\text{Ge}(\text{n},\alpha)^{71\text{m}}\text{Zn}$ ,  $^{74}\text{Ge}(\text{n},\text{np/d})^{73}\text{Ga}$  and  $^{76}\text{Ge}(\text{n},2\text{n})^{75}\text{Ge}$  reactions have been experimentally measured via the activation technique, with the  $^{27}\text{Al}(\text{n},\alpha)^{24}\text{Na}$  reaction used as reference for the determination of the neutron flux. The irradiations were performed at the neutron energy of 15.7 MeV at the recently upgraded neutron beam facility of NCSR "Demokritos". The 5.5 MV Tandem Van de Graaff Accelerator has been upgraded with two new ion sources, a new pelletron charging system, a new gas stripper and beam optics [6].

## 2 Experimental Details

### 2.1 Ge Targets & Reference Foils

Five isotopically enriched Ge targets were employed for the cross-section measurements. The  $^{70,72,73,74,76}\text{Ge}$  targets were provided by the n\_TOF collaboration (CERN) in the form of  $\text{GeO}_2$  pellets of  $\sim 2$  g each, with enrichment levels of 97.71, 96.59, 96.07, 95.51 and 88.46%, respectively. For the neutron flux determination, high purity Al metallic foils of  $\sim 0.4$  g each were used. The Ge targets and the reference foils had a diameter of 20 mm and were glued on a thin mylar foil, fixed on an Al ring.

### 2.2 Neutron beam facility of NCSR "Demokritos"

All the irradiations were performed at the recently upgraded [6] neutron beam facility of NCSR "Demokritos", hosting a 5.5 MV Tandem Van de Graaff accelerator [7]. The quasi- monoenergetic neutron beam was produced at 15.7 MeV via the  $^3\text{H}(\text{d},\text{n})^4\text{He}$  (D-T) reaction. The deuteron beam impinged on a Tritiated Titanium (TiT) target, of 373 GBq activity. The TiT target was placed in an Al flange that was kept in high vacuum during the irradiations and also acted as a Faraday cup for the monitoring of the ion beam charge during the irradiations. The entrance foil of the TiT target was a 10  $\mu\text{m}$  Mo foil, while a 1 mm Cu foil was placed at the back of the target acting as a beam stop. The neutron producing target was water cooled during the irradiations, to avoid any possible thermal damage from the deuteron beam.

### 2.3 Irradiations & Measurements

The duration of the irradiations varied between 5-7 h depending on the half-life of the measured residual nucleus. The fluctuations of the neutron beam during the irradiations were measured with a  $\text{BF}_3$  detector, placed at  $\sim 3$  m from the TiT target and at an angle with respect to the neutron beam, in order to minimize the neutron return to the measuring targets. Each Ge target was placed between two reference Al foils in order to experimentally calculate the neutron flux via the  $^{27}\text{Al}(\text{n},\alpha)^{24}\text{Na}$  reference reaction. Following the irradiations, the induced radioactivity of the residual nuclei was measured via two HPGe detectors of 80% relative efficiency, that were calibrated with a  $^{152}\text{Eu}$  source. The targets and reference foils were measured at a distance of 10 cm from the HPGe detector window, to minimize summing and pile-up effects.

### 3 Data Analysis

The cross section calculation via the activation technique is based on a reference reaction with a well studied cross-section value and is described by equation 1:

$$\sigma = \sigma_{\text{ref}} \cdot \frac{N_{\gamma,\text{tar}}}{N_{\gamma,\text{ref}}} \cdot \left[ \frac{(\varepsilon \cdot F \cdot I_{\gamma} \cdot D \cdot f_c \cdot N_t)_{\text{ref}}}{(\varepsilon \cdot F \cdot I_{\gamma} \cdot D \cdot f_c \cdot N_t)_{\text{tar}}} \right] \cdot \frac{\Phi_{\text{ref}}}{\Phi_{\text{tar}}} \quad (1)$$

In Eq. 1 the factors referring to the measuring targets and reference foils are noted with the subscripts "tar" and "ref" respectively. The cross-section value for the  $^{27}\text{Al}(n,\alpha)^{24}\text{Na}$  reference reaction was obtained from the ENDF/B-VIII.0 library [8], and was found to be 0.099 b with a total estimated uncertainty of 1.7%. The  $\gamma$ -ray used for the neutron flux determination from the  $^{27}\text{Al}(n,\alpha)^{24}\text{Na}$  reference reaction was the 1368.6 keV one. The analysis of all the  $\gamma$ -ray spectra was performed via the "Tv" software [9]. The rest of the factors of equation 1 for the cross section calculation, are described in detail in Ref. [10].

All the factors of equation 1 are considered uncorrelated. Therefore, the final cross-section uncertainty is calculated simply as the quadratic summation of the uncertainty of each factor involved. In many reactions however, two or more  $\gamma$ -rays were used for the cross-section calculation, each providing a different cross-section value ( $\sigma_i$ ) for the measured reaction. In these cases, the final cross section results stem from the weighted average of the different cross-section values calculated ( $\sigma_i$ ), taking into account the correlations between the measurements. For this purpose, equation (27) described in Ref. [11] was used when two  $\gamma$ -rays were used, while the formalism described in Appendix 2 of Ref. [12] was employed, when three  $\gamma$ -rays were used for the calculation of the final cross-section result.

### 4 Simulations

Monte Carlo simulations were necessary for the determination of the neutron flux ratio ( $\frac{\Phi_{\text{ref}}}{\Phi_{\text{tar}}}$ ) in aluminum foils and germanium targets. These simulations were performed with the combined use of NeuSDesc [13, 14] and MCNP5 codes [15]. Firstly, a source definition (SDEF) card was created via the NeuSDesc code, taking into account the characteristics of the Ti/T target (target and entrance foil thickness, Ti/T ratio) along with the straggling of the ion beam in the entrance foil and target implementing the SRIM-2008 code [16] and the kinematics of the D-T neutron producing reaction. This SDEF card was then fed into the MCNP input file, in which the geometry of the experimental setup was accurately described. The propagation of the neutron beam through the stack of reference foils and Ge targets was achieved with the f4 tally (average flux over a volume) scoring.

### 5 Preliminary Results & Discussion

The preliminary cross-section results of the  $^{70}\text{Ge}(n,2n)^{69}\text{Ge}$ ,  $^{72}\text{Ge}(n,p)^{72}\text{Ga}$ ,  $^{72}\text{Ge}(n,\alpha)^{69m}\text{Zn}$ ,  $^{73}\text{Ge}(n,p)^{73}\text{Ga}$ ,  $^{73}\text{Ge}(n,np/d)^{72}\text{Ga}$ ,  $^{73}\text{Ge}(n,\alpha)^{69m}\text{Zn}$ ,  $^{74}\text{Ge}(n,\alpha)^{71m}\text{Zn}$ ,  $^{74}\text{Ge}(n,np/d)^{73}\text{Ga}$  and  $^{76}\text{Ge}(n,2n)^{75}\text{Ge}$  reactions are presented in this section, in Figure 1, along with the experimental data [17] and evaluation libraries [8, 18–22] found in literature. The results of previous measurements from our group (Vlastou et al. [23]) are also presented.

#### 5.1 $^{70}\text{Ge}(n,2n)^{69}\text{Ge}$

The  $^{70}\text{Ge}(n,2n)^{69}\text{Ge}$  reaction produces the  $^{69}\text{Ge}$  residual nucleus that decays to  $^{69}\text{Ga}$  by 100%  $\beta^+$  emission with a half life of 39.05 h. The de-excitation from the different levels of

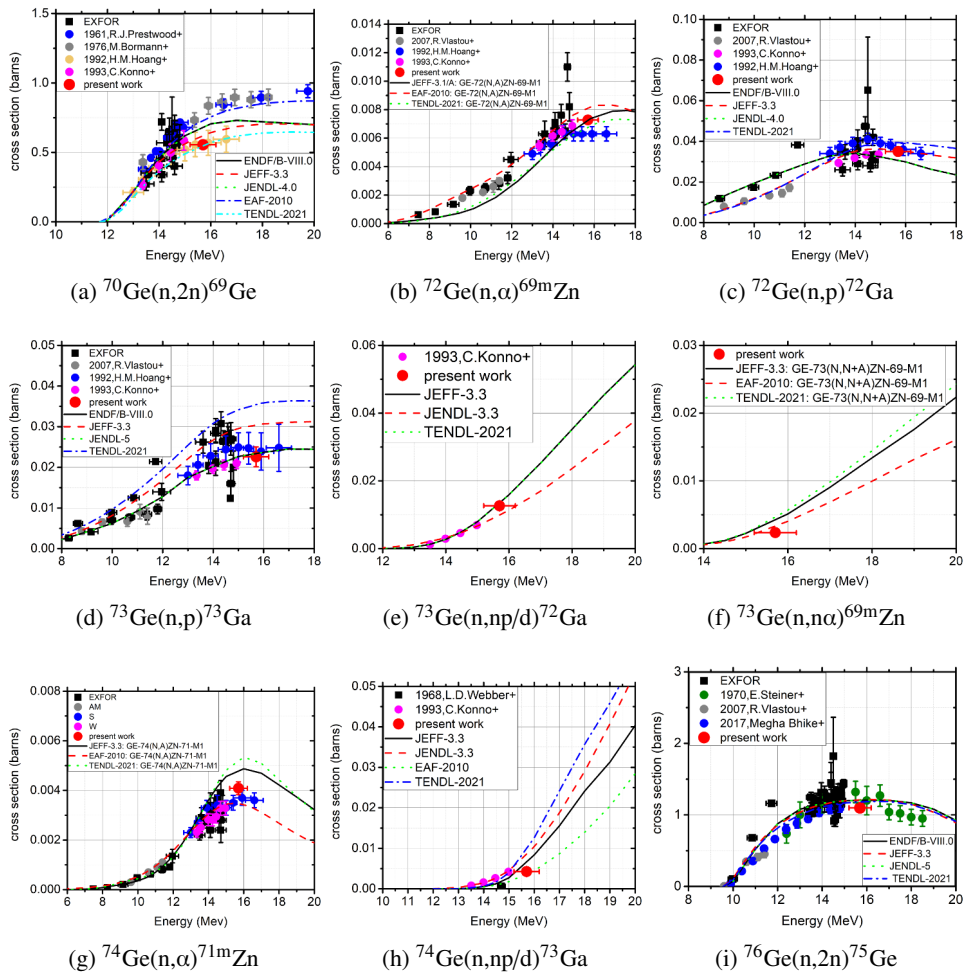


Figure 1: Preliminary results of the measured reactions

the  $^{69}\text{Ga}$  nucleus, produce several  $\gamma$ -rays with the most prominent used in this work being the 1107, 574, 872 and 1337 keV ones with respective intensities of 36.0(4), 13.3(18), 11.9(16) and 4.5(6) % [24]. The preliminary cross-section result presented in Figure 1a, was obtained from the weighted average of the cross-section values calculated from the quite intensive 574 and 872 keV  $\gamma$ -rays, while the respective value calculated from the 1107 and 1337  $\gamma$ -rays was by  $\sim 20\%$  lower. There is an excellent agreement with the dataset of Hoang et al. [25], that also used the 574 keV  $\gamma$ -ray for the cross-section calculation, and the TENDL 2021 [20]. It should be underlined that for this reaction, above 15 MeV two general trends seem to appear. The first with higher cross-section values is followed by the datasets of Prestwood et al. [26], Bormann et al. [27] and the EAF-2010 library [22]. The second one is followed by the results of the present work, the dataset of Hoang et al. and the TENDL-2021 and the JEFF-3.3 libraries [18]. The discrepancies between these two trends could be attributed to the large uncertainties of the  $\gamma$ -ray intensity ( $I_\gamma$  factor), ranging from 11 to 14 % for the most prominent  $\gamma$ -rays emitted from the  $^{69}\text{Ge}$  residual nucleus.

## 5.2 $^{72}\text{Ge}(\text{n},\alpha)^{69\text{m}}\text{Zn}$

The  $^{72}\text{Ge}(\text{n},\alpha)$  reaction produces the  $^{69}\text{Zn}$  residual nucleus in both its ground and isomeric state. The isomeric state is the only one studied via the activation technique in the present work. It decays to the respective ground state (99.97% IT) with a half life of 13.76 h, emitting the characteristic 438.6 keV  $\gamma$ -ray with an intensity of 94.85(7)% [24]. The preliminary cross-section result of the present work is presented in Figure 1b. It is in excellent agreement with the dataset of Konno et al. [28], in which an isotopically enriched Ge target was also used, as well as with the trend of TENDL-2021 [20] and JEFF-3.1/A [21] evaluated libraries. The dataset of Hoang et al. which is the only one exceeding 15 MeV neutron energy seems to slightly underestimate the cross-section values.

## 5.3 $^{72}\text{Ge}(\text{n},\text{p})^{72}\text{Ga}$

The  $^{72}\text{Ge}(\text{n},\text{p})^{72}\text{Ga}$  reaction produces the  $^{72}\text{Ga}$  residual nucleus that decays via 100%  $\beta^-$  decay and with a half life of 14.1 h, to  $^{72}\text{Ge}$ . The de-excitation of this nucleus to its ground state is accompanied by the emission of many  $\gamma$ -rays, with some of the most prominent ones being the 834.13, 629.97 and 894.33 keV with respective intensities 95.45(8), 26.13(4) and 10.136(15)% [29]. The cross-section result of the present work was calculated as the weighted average of the three different corresponding cross-section values, taking into account the respective correlations as described in section 3. This result, presented in Figure 1c, is in excellent agreement with the dataset of Konno et al., and the dataset of Hoang et al., within the statistical uncertainties of the measurements.

## 5.4 $^{73}\text{Ge}(\text{n},\text{p})^{73}\text{Ga}$

The  $^{73}\text{Ge}(\text{n},\text{p})^{73}\text{Ga}$  reaction produces the  $^{73}\text{Ga}$  residual nucleus that decays (100%  $\beta^-$ ) to  $^{73}\text{Ge}$  with a half life of 4.86 h. The de-excitation of  $^{73}\text{Ge}$  to its ground state produces the 297.38 and 325.73 keV  $\gamma$ -rays, with corresponding intensities of 79.8(19)% and 11.2(4)% [30]. The cross-section result obtained from the weighted average of the two characteristic  $\gamma$ -rays is presented in Figure 1d. There is an excellent agreement between the result of the present work and the ones from the datasets of Konno et al. (with an enriched target) and the dataset of Hoang et al. within the statistical uncertainties of the measurements, as well as the ENDF/B-VIII.0 [8] and JENDL-5 [19] evaluation libraries.

## 5.5 $^{73}\text{Ge}(\text{n,np/d})^{72}\text{Ga}$

The  $^{73}\text{Ge}(\text{n,np/d})^{72}\text{Ga}$  reaction produces the  $^{72}\text{Ga}$  residual nucleus. The decay properties of this nucleus and the  $\gamma$ -rays used for the cross-section calculation are described in section 5.3. The result of the present work that is presented in Figure 1e, is in very good agreement with the dataset of Konno et al., which is the only one found in literature for this reaction. The JEFF-3.3 and TENDL-2019 libraries are also in very good agreement with the result of the present work.

## 5.6 $^{73}\text{Ge}(\text{n,n}\alpha)^{69\text{m}}\text{Zn}$

The  $^{73}\text{Ge}(\text{n},\text{n}\alpha)$  reaction produces the  $^{69}\text{Zn}$  residual nucleus in both its ground and isomeric state. The decay properties of this nucleus and the  $\gamma$ -ray used for the cross section determination are described in section 5.2. No other experimental data were found for this reaction, while the existing evaluation libraries [18, 20, 22], in lack of sufficient number of experimental points, seem to underestimate the cross-section values.

### 5.7 $^{74}\text{Ge}(\text{n},\alpha)^{71\text{m}}\text{Zn}$

The  $^{74}\text{Ge}(\text{n},\alpha)$  reaction produces the  $^{71}\text{Zn}$  residual nucleus in both the ground and an isomeric state. Only the latter is studied in this work that decays via 100%  $\beta^-$  decay to  $^{71}\text{Ga}$  with a half life of 4.14 h. The de-excitation to its respective ground state is accompanied by the emission of the 386.28 and 487.34 keV  $\gamma$ -rays with respective intensities of 89.0(11)% and 61.9(4)% [31]. The preliminary cross-section results that are presented in Figure 1g are in very good agreement with the trend of the dataset of Konno et al. and the cross-section values of Hoang et al., within the statistical uncertainties. The existing libraries above 15 MeV are quite discrepant, possibly due to the lack of experimental data in this energy region.

### 5.8 $^{74}\text{Ge}(\text{n,np/d})^{73}\text{Ga}$

The decay properties of the  $^{73}\text{Ga}$  residual nucleus produced from the  $^{74}\text{Ge}(\text{n,np/d})^{73}\text{Ga}$  reaction, are described in section 5.4. The preliminary cross-section result of the present work is presented in Figure 1h and is in good agreement with the EAF-2010 evaluation library, while the trend of the dataset of Konno et al. seems to slightly overestimate the cross-section values.

### 5.9 $^{76}\text{Ge}(\text{n,2n})^{75}\text{Ge}$

The  $^{76}\text{Ge}(\text{n,2n})^{75}\text{Ge}$  reaction produces the  $^{75}\text{Ge}$  residual nucleus that decays to  $^{75}\text{As}$  (100%  $\beta^-$ ). The de-excitation to the ground state of  $^{75}\text{As}$ , is accompanied by the emission of the 264.6 and 198.6 keV  $\gamma$ -rays with respective intensities of 11.4(11)% and 1.19(12)% [32]. The preliminary cross-section result are presented in Figure 1i and are in very good agreement with the trend of all the presented libraries as well as with the dataset of Megha Bhike et al. [33] that also used an enriched target for the measurements, and the dataset of Steiner et al. [34] which is the only one in the energy range above 15 MeV.

## 6 Summary

The preliminary cross-section results of the  $^{70}\text{Ge}(\text{n,2n})^{69}\text{Ge}$ ,  $^{72}\text{Ge}(\text{n,p})^{72}\text{Ga}$ ,  $^{72}\text{Ge}(\text{n},\alpha)^{69\text{m}}\text{Zn}$ ,  $^{73}\text{Ge}(\text{n,p})^{73}\text{Ga}$ ,  $^{73}\text{Ge}(\text{n,np/d})^{72}\text{Ga}$ ,  $^{73}\text{Ge}(\text{n},\alpha\alpha)^{69\text{m}}\text{Zn}$ ,  $^{74}\text{Ge}(\text{n},\alpha)^{71\text{m}}\text{Zn}$ ,  $^{74}\text{Ge}(\text{n,np/d})^{73}\text{Ga}$  and  $^{76}\text{Ge}(\text{n,2n})^{75}\text{Ge}$  reactions are presented for neutron energy of 15.7 MeV, where few experimental data exist and the evaluation libraries exhibit discrepancies. The isotopically enriched Ge samples used in the present work were provided by the n\_TOF collaboration (CERN) in the form of  $\text{GeO}_2$  pellets. The cross-section results produced from enriched targets are more accurate in comparison with the ones produced from  $^{nat}\text{Ge}$  targets, since in the latter case, the measured yield is "contaminated" by other reaction channels stemming from neighboring isotopes that exist in the  $^{nat}\text{Ge}$  target in their natural abundances. This contribution becomes significant for neutron energies above  $\sim$ 14 MeV. Accurate cross section values measured with highly enriched targets are thus very important in this energy range, since the aforementioned "contamination" is negligible. Therefore, these cross-section results could act as a very important constraint in the input parameters of statistical model calculations, and could improve the accuracy of future evaluation libraries.

## Acknowledgments

We acknowledge support of this work by the project CALIBRA/EYIE (MIS 5002799), which is implemented under the Action Reinforcement of the Research and Innovation Infrastructures, funded by the Operational Program Competitiveness, Entrepreneurship and Innovation

(NSRF 2014-2020) and co-financed by Greece and the European Union (European Regional Development Fund)

The research work was supported by the Hellenic Foundation for Research and Innovation (HFRI) under the 3rd Call for HFRI PhD Fellowships (Fellowship Number: 5597).

Funded by the Basic Research Program PEVE 2021 of the National Technical University of Athens.

## References

- [1] M. Avrigeanu, V. Avrigeanu, M. Diakaki, R. Vlastou, *Physical Review C* **85**, 44618 (2012)
- [2] A. Fessler, A.J. Plomp, D.L. Smith, J.W. Meadows, Y. Ikeda, *Nuclear Science and Engineering* **134**, 171 (2000)
- [3] P. Talou, T. Kawano, P.G. Young, M.B. Chadwick, R.E. MacFarlane, *Nuclear Science and Engineering* **155**, 84 (2007)
- [4] N. Dzysiuk, A. Koning, *EPJ Web of Conferences* **146**, 2047 (2017)
- [5] A. Tsinganis, M. Diakaki, M. Kokkoris, A. Lagoyannis, E. Mara, C.T. Papadopoulos, R. Vlastou, *Physical Review C* **83**, 24609 (2011)
- [6] A. Lagoyannis, M. Andrianis, M. Axiotis, P. Chatzispyroglou, S. Harissopoulos, A. Laoutaris, I.E. Stamatelatos, T. Tsiamis, *HNPS Advances in Nuclear Physics* **29**, 3337 (2023)
- [7] S. Harissopoulos, M. Andrianis, M. Axiotis, A. Lagoyannis, A.G. Karydas, Z. Kotsina, A. Laoutaris, G. Apostolopoulos, A. Theodorou, T.J.M. Zouros et al., *The European Physical Journal Plus* **136**, 617 (2021)
- [8] D.A. Brown, M.B. Chadwick, R. Capote, A.C. Kahler, A. Trkov, M.W. Herman, A.A. Sonzogni, Y. Danon, A.D. Carlson, M. Dunn et al., *Nuclear Data Sheets* **148**, 1 (2018)
- [9] J. Theuerkauf, S. Esser, S. Krink, M. Luig, N. Nicolay, O. Stuch, H. Wolters, *Program Tv* (Institute for Nuclear Physics, Cologne, 1993), <https://www.ikp.uni-koeln.de/~fitz/viewspectra/viewspectra.html>
- [10] Chasapoglou, S., Vlastou, R., Kokkoris, M., Diakaki, M., Michalopoulou, V., Gkatis, G., Stamatopoulos, A., Axiotis, M., Harissopoulos, S., Lagoyannis, A. et al., *EPJ Web of Conf.* **284**, 01003 (2023)
- [11] N. Otuka, B. Lalremruata, M. Khandaker, A. Usman, L. Punte, *Radiation Physics and Chemistry* **140**, 502 (2017)
- [12] W. Mannhart, *A Small Guide to Generating Covariances of Experimental Data (INDC(NDS)-0588)* (2011)
- [13] E. Birgersson, G. Loevestam, *NeuSDesc-Neutron Source Description Software Manual. EUR 23794 EN* (OPOCE, Luxembourg (Luxembourg), 2009), <https://publications.jrc.ec.europa.eu/repository/handle/JRC51437>
- [14] B. Evert, L. Goeran, Technical Report, EUR 23794 EN (European Comission) (2009)
- [15] X-5 Monte Carlo team, *MCNP - A General Monte Carlo N-Particle Transport Code, version 5 - LA-UR-03-1987* (2003 - Rev. 2008)
- [16] J. Ziegler, J. Biersack, M. Ziegler, *SRIM, the Stopping and Range of Ions in Matter* (SRIM Company, 2008), ISBN 9780965420716
- [17] N. Otuka, E. Dupont, V. Semkova, B. Pritychenko, A. Blokhin, M. Aikawa, S. Babykina, M. Bossant, G. Chen, S. Dunaeva et al., *Nuclear Data Sheets* **120**, 272 (2014)

- [18] A.J.M. Plompen, O. Cabellos, C. De Saint Jean, M. Fleming, A. Algora, M. Angelone, P. Archier, E. Bauge, O. Bersillon, A. Blokhin et al., The European Physical Journal A **56**, 181 (2020)
- [19] K. Shibata, O. Iwamoto, T. Nakagawa, N. Iwamoto, A. Ichihara, S. Kunieda, S. Chiba, K. Furutaka, N. Otuka, T. Ohsawa et al., Journal of Nuclear Science and Technology **48**, 1 (2011)
- [20] A. Koning, D. Rochman, J.C. Sublet, N. Dzysiuk, M. Fleming, S. van der Marck, Nuclear Data Sheets **155**, 1 (2019), special Issue on Nuclear Reaction Data - Rev. 2021 [https://tendl.web.psi.ch/tendl\\_2021/tendl2021.html](https://tendl.web.psi.ch/tendl_2021/tendl2021.html)
- [21] A. Koning, R. Forrest, M. Kellett, R. Mills, H. Henriksson, Y. Rugama, O. Bersillon, O. Bouland, A. Courcelle, M.C. Duijvestijn et al., Tech. Rep. 92-64-02314-3, Nuclear Energy Agency of the OECD (NEA) (2006)
- [22] J.C. Sublet, L.W. Packer, J. Kopecky, R.A. Forrest, A.J. Koning, D.A. Rochman, CCFE-R **10**, 05 (2010)
- [23] R. Vlastou, C.T. Papadopoulos, M. Kokkoris, G. Perdikakis, S. Galanopoulos, M. Serris, A. Lagoyannis, S. Harissopoulos, Journal of Radioanalytical and Nuclear Chemistry **272**, 219 (2007)
- [24] C. Nesaraja, Nuclear Data Sheets **115**, 1 (2014)
- [25] H.M. Hoang, U. Garuska, D. Kielan, A. Marcinkowski, B. Zwieglinski, Zeitschrift für Physik A Hadrons and Nuclei **342**, 283 (1992)
- [26] R.J. Prestwood, B.P. Bayhurst, Phys. Rev. **121**, 1438 (1961)
- [27] M. Bormann, H.K. Feddersen, H.H. Hölscher, W. Scobel, H. Wagener, Zeitschrift für Physik A Atoms and Nuclei **277**, 203 (1976)
- [28] C. Konno, Y. Ikeda, K. Kawade, H. Yamamoto, H. Maekawa, JAERI Reports-1329 (1993)
- [29] D. Abriola, A. Sonzogni, Nuclear Data Sheets **111**, 1 (2010)
- [30] B. Singh, J. Chen, Nuclear Data Sheets **158**, 1 (2019)
- [31] B. Singh, J. Chen, Nuclear Data Sheets **188**, 1 (2023)
- [32] A. Negret, B. Singh, Nuclear Data Sheets **114**, 841 (2013)
- [33] M. Bhike, Krishichayan, W. Tornow, Phys. Rev. C **95**, 054605 (2017)
- [34] E. Steiner, P. Huber, W. Salathe, R. Wagner, Helv. Phys. Acta **43**, 17 (1970)